Journal of Nondestructive Evaluation, Vol. 7, No. 1, 1987

Laser Excitation Through Fiber Optics for NDE

C. P. Burger,[1] T. D. Dudderar,[2] J. A. Gilbert,[3] B. R. Peters,[3] and J. A. Smith[1]

Received November 20, 1986; revised March 26, 1987

This paper describes experiments designed to generate acoustic waves by using a laser pulse, transmitted through fiber optics, to thermally shock the surface of a steel specimen. The purpose of this effort was to explore the noncontacting generation of Rayleigh surface waves appropriate to the interrogation of structures for the detection of subcritical defects, with the ultimate goal of developing an efficient laser-based nondestructive evaluation technique utilizing flexible fiber optics.

KEY WORDS: Ultrasonics; fiber optics; lasers.

1. INTRODUCTION

The goal of the engineering research program on laser excitation for nondestructive evaluation is to explore the synthesis of fiber-optic/high-power laser excitation systems with sophisticated detection techniques to inspect, locate, and characterize internal structural defects in normally inaccessible components. This approach will generate its excitation by guiding high-energy laser pulses through a remotely controlled fiber-optic probe to an appropriate location on the test structure where the output is focused onto a surface. The resulting thermal shocks produce both acoustic (mechanical) and thermal (temperature) waves which interrogate the structure. After interacting with a defect the modified responses can be monitored by standard acoustic-wave or ultrasonic detection techniques or thermal-transient detection systems.

It is intended to eventually develop a flaw-detection technique with the capacity, through the use of flexible fiber optics, of reaching and exciting otherwise inaccessible regions of a structure. In addition, this technique will utilize one means of excitation, focused high-energy laser pulses, to generate two types of signals with different propagation characteristics, one of them acoustic and the other thermal, which can be detected and evaluated separately. Finally, since it will not require the mechanical coupling of an excitation transducer to the surface of the test structure, it will have an advantage over traditional piezoelectric transducer-based ultrasonic testing techniques which can be very difficult to apply to structures with complex surface geometries. Consequently, it is anticipated that this technique, if successful, would be of great value in the inspection of many structures where conventional methods of flaw detection are not appropriate, such as aircraft engines, nuclear reactor pressure vessels, and similar enclosed assemblies with limited access.

2. OBJECTIVES

The primary objective of this initial research program was to demonstrate the feasibility of gener-

[1] Mechanical Engineering Department, Texas A&M University, College Station, Texas 77843.
[2] Bell Laboratories, Murray Hill, New Jersey 07974.
[3] Dept. of Mechanical Engineering, University of Alabama-Huntsville, Huntsville, Alabama 35899.

0195-9298/87/0300-0057$05.00/0

ating acoustic (mechanical, ultrasonic) waves in a metal specimen by impacting its surface with a laser pulse delivered through a flexible optical fiber element and recording the resulting Rayleigh surface wave with a standard piezoelectric *R*-wave transducer and wedge. The second objective was to demonstrate the detection of a "flaw" in the metal bar through the use of the above fiber-optic excitation system and a standard piezoelectric transducer detector. Subsequent efforts will be focused on exploring the thermal wave aspects of this approach using real-time infrared imaging techniques.

2.1. Generating an Acoustic Wave with a Laser Pulse

In order to establish a reference system a pitch–catch arrangement for both input and output through piezoelectric-type *R*-wave transducers was set up as shown in Fig. 1(a). Figure 1(b) shows the equivalent set-up with a direct laser-pulse input and a piezoelectric output while Fig. 1(c) shows the same set-up with the laser pulse input through a flexible fiber-optic component. The instrumentation set-ups for each mode of operation are shown schematically in Fig. 2. None employed a preamplifier between the receiving transducer and the oscilloscope. The paired piezoelectric-transducer arrangement of Fig. 1(a) and Fig. 2(a) was used extensively to characterize different trigger and recording set-ups. When the distance, b_1, (see Fig. 1(a)) between the transducer faces in this setup was reduced to zero, the initial delay "between the input pulse to the sending transducer and the output pulse from the receiving transducer" was found to be 20 μs. This delay was associated with the acoustic path length between the piezoelectric elements mounted on Lucite wedges which make up the transducers. Since the geometrics of these transducers are identical, it is reasonable to assign half of this acoustic path length to each. In the subsequent

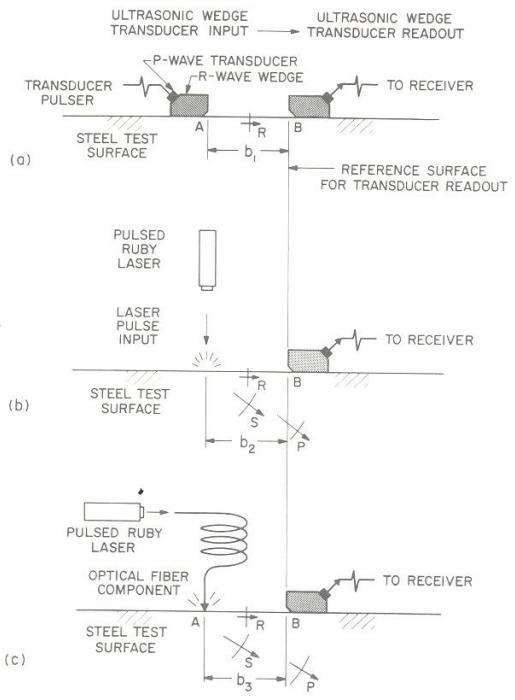

Fig. 1. Diagram of piezoelectric transducer and *R*-wedge calibration for ultrasonic wave detection system: (a) with a piezoelectric transducer and *R*-wedge input (ultrasonic pitch–catch set-up), (b) with a direct laser pulse input, (c) with a laser pulse input through an optical-fiber component.

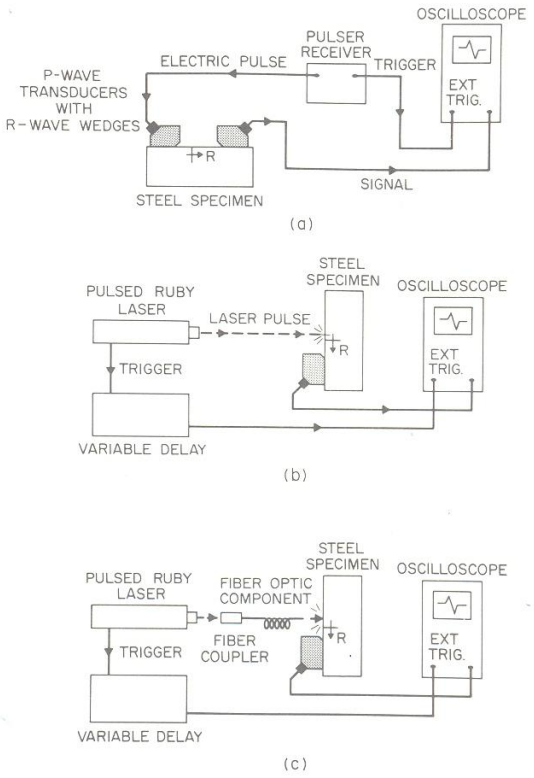

Fig. 2. Schematic of the instrumentation: (a) with the ultrasonic pitch–catch set-up, (b) with the direct laser pulse input, (c) with the laser pulse input through an optical-fiber component.

experiments with laser excitation the origin of the acoustic wave was taken to be time zero. This coincides with the arrival of the light pulse at the surface of the metal to within a few nanoseconds. Consequently, for all time-of-flight measurements from the laser input to the measured pulse in the set-up of Figs. 1(b) and 2(b) a delay of half the initial delay, 10 μs, was subtracted from the time base on the oscilloscope screen to provide the appropriate correction to the signal. The travel time for an R-wave across distance b_2 on Fig. 1(b) would be simply

$$t = (b_2/C_R)$$

where C_R is the appropriate R-wave velocity. Because the delays in the optical-fiber elements used in the subsequent tests of the type shown in Fig. 1(c) were relatively insignificant, the same 10 μs time base correction was used there also.

All specimens were AISI 1020 steel bars (25.4 mm $\times$ 25.4 mm $\times$ 203.2 mm) with normal "as-machined" surfaces and no special surface treatments except where otherwise described. The R-wave velocity, C_R, in the steel was measured at 2.96 mm/μs which is reasonably approximated as $C_R = 3$ mm/μs for convenience.

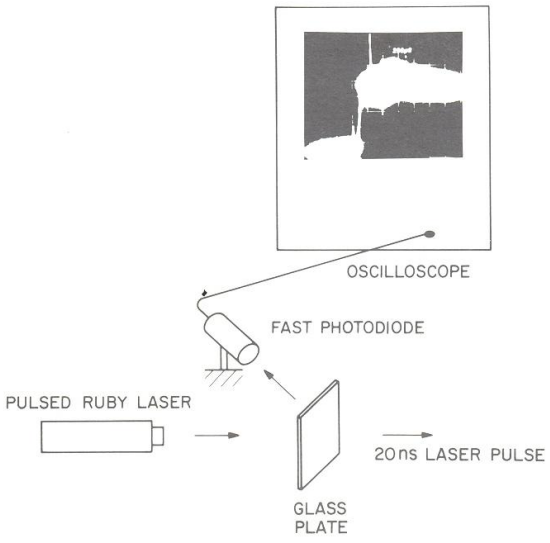

Fig. 3. Laser pulse detection arrangement showing intensity response at high sensitivity (50 mV/div at 200 μS/div). Here the laser pulse spike extends far off the oscilloscope screen.

The time-history of the light pulse from the laser and the set-up used to record it are shown in Fig. 3. Since a direct pulse would have damaged the photodiode, this recording was made from the front surface reflections off a glass plate. Time zero in Fig. 3 is the time of the trigger to the laser, and the first spike at 600 μs is the ignition firing. The trace shows the light-intensity variation as the flash lamp charges and holds for the next 220 μs until the laser fires at 820 μs. The resulting 20-nanosecond high-energy (3 to 6 Joules at the laser) spike carries the trace far off the scale on this photograph. The trailing features after laser firing are possibly due to ringing in the diode.

2.2. Excitation with a Direct Laser Pulse

The first series of tests were conducted using the configuration of Fig. 1(b) to explore the use of laser pulses to generate detectable elastic waves in the test bar following the work of many researchers as reviewed elsewhere.[1-4] The effects of varying the "illuminated" spot size and intensity (power) were determined by placing a beam-limiting aperture and a long focal-length lens in the path of the laser pulses (to converge the "beam" as shown in Fig. 4). By appropriately varying the distance of the specimen and the size of the aperture it was possible to achieve a variety of input conditions and observe the corresponding responses of the piezoelectric transducer detector. Apertures of 20 mm, 5 mm and 1 mm diameter were used to vary the input power. Figure 5 shows typical signals from a selection of aperture- and effective-illuminated spot size combinations.

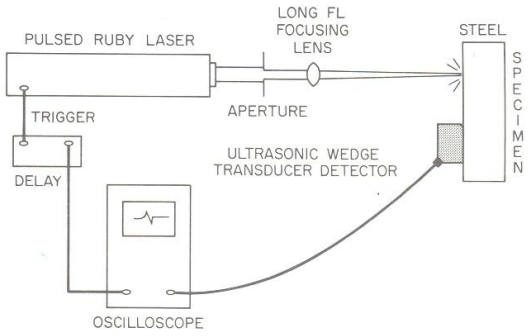

Fig. 4. Diagram of the system used to vary the illumination spot size and the power of the laser pulse.

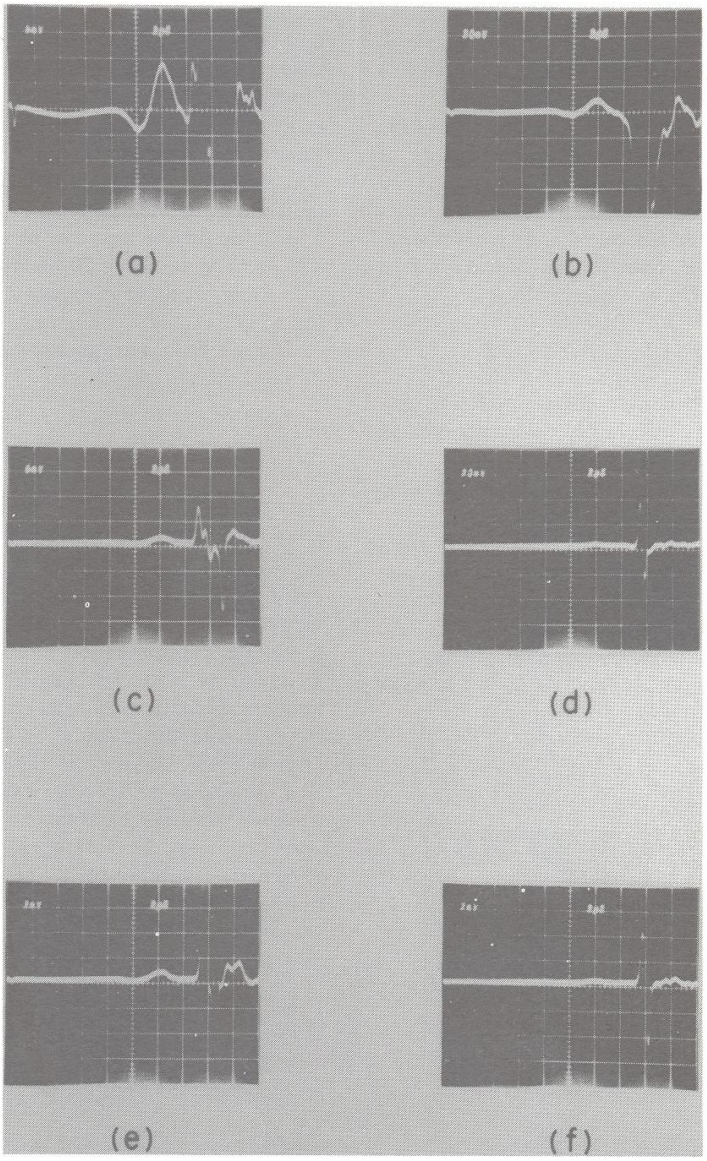

Fig. 5. Oscilloscope traces showing the *R*-wave response at 2 μS/div from the piezoelectric transducer/detector for a laser pulse transmitted through: (a) 20 mm aperture to a 5 mm diameter spot (with a sensitivity of 5 mV/div), (b) 20 mm aperture to a 1 mm diameter spot (with a sensitivity of 20 mV/div), (c) 5 mm aperture to a 5 mm diameter spot (with a sensitivity of 5 mV/div), (d) 5 mm aperture to a 1 mm diameter spot (with a sensitivity of 20 mV/div), (e) 5 mm aperture to a 2.5 mm diameter spot (with a sensitivity of 2 mV/div), (f) 1 mm aperture to a 1 mm diameter spot (with a sensitivity of 2 mV/div).

From these results it can be seen that, within the range of power densities employed here, the wave shape depends strongly on the input spot size and rather less so on the power, with the cleanest Rayleigh wave shape appearing when the illuminated spot was around 1 mm in diameter.[5]

In all cases the input conditions were in the thermoelastic range, i.e. all effects were caused by thermoelastic phenomena rather than the so-called plasma phenomenon where ablations, melting, and so forth occur at the point of "laser impact."

2.3. Excitation through a Flexible Optical-Fiber Element

With the conditions for generating clean Rayleigh waves established, a second series of tests were conducted to explore the use of fiber-optic components to deliver laser pulses appropriate to the generation of comparable quality waves. Using the configuration shown in Fig. 6(a) both single optical fibers and flexible optical-fiber bundles were evaluated. Again, the target surface was the shiny, "as-machined" surface on the same steel bar specimen used in all the previous tests.

Operationally, the unprotected input end of the optical fiber or optical-fiber bundle proved to be highly vulnerable to damage due to the high energy densities in the focused pulse at the point of launch. Following Bjelkhagen[5] the specially-built device shown in Fig. 6(b) was employed to provide a more robust coupling. This device consisted of a plane quartz window (or a planoconcave collimating lens) at the input end which directed the incoming pulse onto the end of the fiber-optic bundle (or single optical fiber) through a cell which could be filled with an index-matching fluid (a fluid that matched the index of refraction of the fibers). Both Cargille Laboratories Code 50350 immersion liquid and pure olive oil were used successfully. This fluid cell was made larger enough to that the absorbed energy from the laser pulses did not excessively heat the fluid.

Figure 7(a) shows the results recorded with the set-up of Fig. 6(a). Here the laser pulse was launched into and guided through a 2 mm diameter fiber-optic

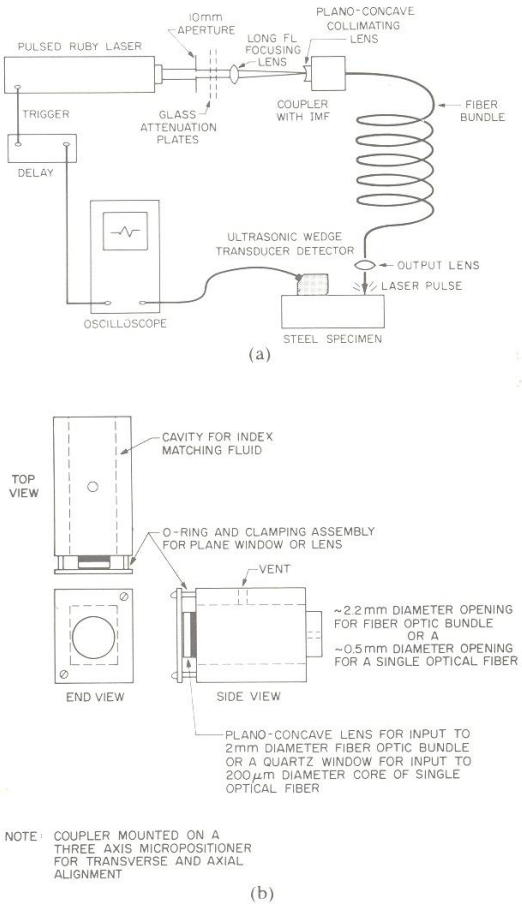

Fig. 6. (a) Schematic diagram of the system used to transmit a 20 ns laser pulse through an optical fiber bundle to the steel bar specimen and to detect the resulting acoustic wave in the specimen, (b) detail of the coupler used in Fig. 6(a).

bundle with its output focused through an output lens onto a 1 mm-diameter spot on the surface of the specimen. It can be seen in this trace that the quality of the resulting wave was quite good; cleaner, in fact, than the Rayleigh wave fronts usually generated by wedge-mounted transducers. When the surface of the specimen was artificially blackened in an effort to enhance coupling energy into the metal and increase amplitude, the wave-shape changed to that shown in Fig. 7(b). In this case the phenomena that generate the elastic wave were no longer purely thermoelastic, but included impact from the ablation of the surface coating, with an obviously less satisfactory result.

[5] The effective-illuminated spot size was estimated from the diameter of the "white burn" that appeared on a previously developed unexposed (all black) polaroid print when it was placed at the point of impact and illuminated by the focused laser pulse.

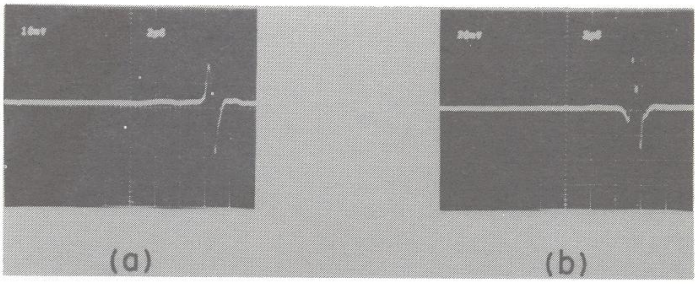

Fig. 7. Oscilloscope traces showing the response at 2 μS/div from the piezoelectric transducer/detector with the specimen excited by laser pulses transmitted through a fiber-optic bundle and focused to a 1 mm diameter spot: (a) on a shiny, as-machined surface (with a sensitivity of 10 mV/div), (b) on the same surface painted black (with a sensitivity of 20 mV/div).

Finally, the fundamental transmission efficiency of a fiber-optic bundle is lower than that of a single low-loss optical fiber. Coupling into a fiber-optic bundle with 2 mm diameter is, however, far easier than coupling into the much smaller core of a single optical fiber. Consequently, only if the laser pulse is focused very accurately onto the core of the single optic-fiber will the greater overall efficiency of a single optic fiber be realized. In such a situation longer lengths of a smaller-diameter, more-flexible single optic fiber can be used, which is highly desirable in applications to remote inspection. In order to test the feasibility of using a single moderately low-loss (9.67 db/km) multimode optical fiber to transmit the laser pulses, the set-up of Fig. 6 was modified for coupling to a 0.25 mm-diameter optical fiber with a single 200 μm core (see Fig. 8). Since the numerical aperture of the optical fiber was around 0.25 at the operating wavelength, no output lens was needed to

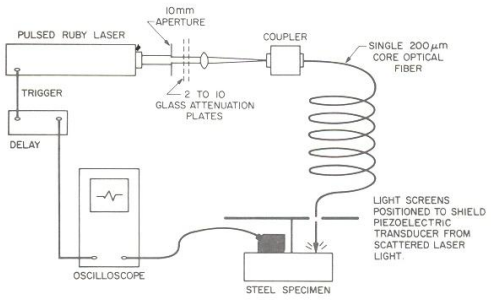

Fig. 8. Schematic diagram of the system shown in Fig. 6(a) modified for use with a single optical fiber.

focus the illumination from the optical fiber onto the metal specimen. A spot size of 1 mm was easily achieved at a reasonable (~ 2 mm) stand-off distance between the optical fiber tip and the specimen surface.

During preliminary single-optical-fiber tests it was found to be very difficult (if not impossible) to align optical fibers with very small core diameters (7 μm single mode or 50 μm multimode) with enough accuracy to achieve usable coupling, with or without index matching fluids. Moreover, while it worked well with a CW laser beam, the existing system could not provide consistently accurate coupling of the pulsed ruby-laser output even into the optical fiber with the much larger 200 μm diameter core. Consequently, the system was significantly less efficient than it might have been. As a result, it generated *R*-waves of much smaller amplitude than those seen in the previous tests with the 2 mm-diameter fiber-optic bundle. Interestingly, at the high gains used in the process of measuring the shapes of these much weaker waves, it was found that the Lucite wedge of the ultrasonic transducer passed light scattered from the vicinity of the impact point to the piezoelectric transducer. This light somehow excited the crystal itself, thereby creating "noise" in the oscilloscope trace during the initial few microseconds after the laser was triggered. Figure 9(a) shows this noise and also suggests that, under certain circumstances, this effect can distort the *R*-wave signal. When the transducer was optically screened from the light both the initial noise and the apparent distortions disappeared and a clean signal was obtained as shown in Fig. 9(b). Note that the vertical scale on these figures is

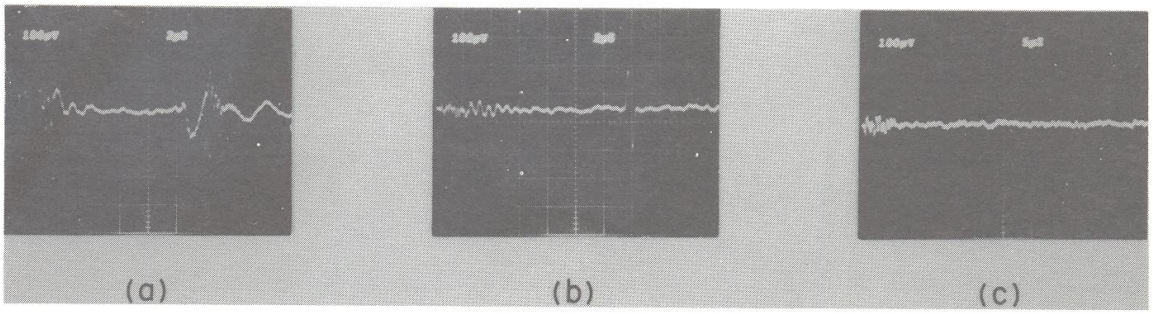

Fig. 9. Oscilloscope traces showing the response (with a sensitivity of 100 mV/div at 2 μS/div) from the detector circuit with noise preceding the arrival of the *R*-wave at the piezoelectric transducer recorded using the set-up shown in Fig. 8: (a) without the light screens, (b) with the light screens, (c) with the light screens and blocked output from fiber (no acoustic wave is generated and no signal is detected).

100 times more sensitive than in Fig. 7(a). The low-level noise still present in the first 6 μs of Fig. 9(b) is from electromagnetic interference caused by the discharge processes of the pulsed laser itself. For Fig. 9(c) the experimental set-up was exactly the same as for Figs. 9(a) and 9(b) except that the light pulse from the laser was interrupted before striking the specimen. There is no sign of an elastic wave but the electromagnetic interference is still present. Because of its timing and limited duration this interference was not found to be bothersome, and no further effort was made to screen the detector system from the laser and its associated electronics from electromagnetic interference.

At full power (~ 6 J) the focused laser pulse would damage the input end of the optical fiber. To prevent such an occurrence, the laser was always operated at its minimum functional power lever (~ 3 J) and attenuation plates of clear glass were inserted between the laser and the focusing lens. In this way the effective power launched into the optical fiber and eventually reaching the specimen was significantly reduced and could easily be varied by adding or subtracting plates. Finally, while the present tests demonstrate that both optical-fiber bundles and single optical fibers can be used, the problem of achieving an efficient coupling into the core of the single optical fiber must be solved if the advantages of such single optical-fiber systems are to be realized. In the absence of such an optimized coupling technique the flexible fiber-optic bundle with an appropriately focused output clearly provides the most practical means of delivering high-intensity pulses of laser light to the impact point.

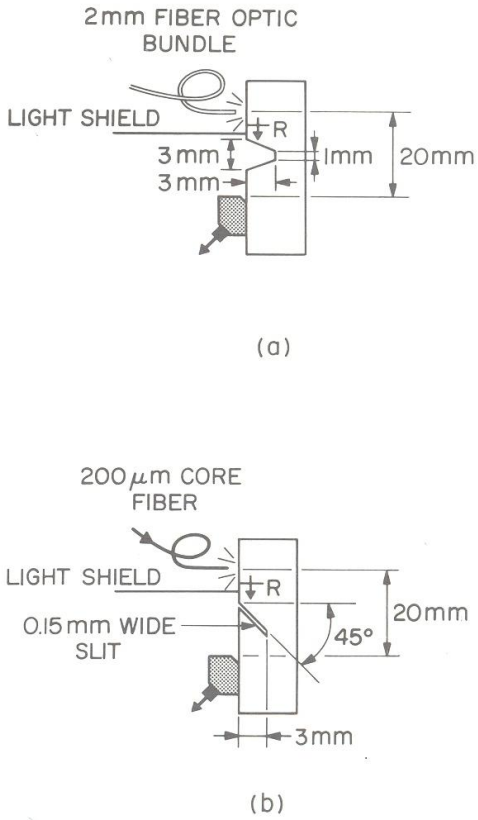

Fig. 10. Diagram showing steel bar specimens with simulated "flaws" for tests with the laser pulses transmitted through: (a) a 2 mm diameter fiber optic bundle, (b) a single fiber with a 200 μm core diameter.

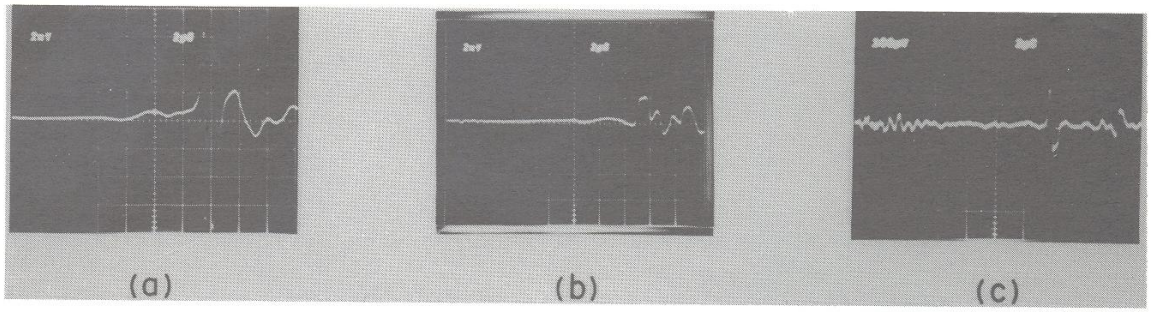

Fig. 11. Oscilloscope traces (at 2 μS/div) showing the effects of the interactions between the *R*-wave and steel bar specimens with: (a) the fiber-optic bundle and no "flaw" (with a sensitivity of 2 mV/div), (b) the fiber-optic bundle and a *V*-notch "flaw" (with a sensitivity of 2 mV/div), (c) the single optical fiber and a slanting slit "flaw" (with a sensitivity of 100 mV/div).

2.4. Evaluating the Interaction Between an Optically-Generated Rayleigh Wave and a Defect

In order to test the capacity of waves generated by a laser pulse transmitted through a flexible optical-fiber bundle to interrogate metal components for defects, 25.4 mm × 25.4 mm × 203.2 mm steel bar specimens with artificially-produced surface "flaws" were tested. These specimens are shown in Fig. 10 and the results are shown in the sequence of photographs of Fig. 11.

Figure 11(a) shows the reference signal for the test depicted in Fig. 10(a) but with the specimen positioned so that there is no "flaw" between the input and readout points. In contrast, the result when there is a "flaw" between the impact point and the transducer (Fig. 10(a)) is shown in Fig. 11(b). This trace displays the classical double wave response associated with the interaction between a Rayleigh wave and a shallow notch.

Finally, the ability of a wave generated from a much lower-intensity laser pulse output from a single fiber to interrogate a test bar with a shallow surface slit, Fig. 10(c), is demonstrated as the trace shown in Fig. 11(c).

Once again, the trace is as expected for the transmitted Rayleigh wave after interacting with a slanting surface "crack."

3. SUMMARY AND CONCLUSIONS

The present study has demonstrated the feasibility of using 20 ns laser pulses transmitted through flexible optical-fiber elements to excite acoustic waves in a metal specimen, and that such waves may be used to detect flaws in much the same way such waves are used to detect flaws in the standard ultrasound technique. Further work will address the use of real-time IR-imaging techniques to sense the accompanying thermal transient, with the ultimate objective being the realization of a flexible fiber-optic system for exciting metal structures for interrogation by complementary acoustic and thermal wave techniques.

ACKNOWLEDGMENTS

The authors wish to thank Iowa State University, AT&T Bell Laboratories, The University of Alabama at Huntsville, and the U.S. Army Research Office under grants DAAG 29-85-K-0178 and DAAG 29-84-K-0183 for their support of this effort.

REFERENCES

1. C. B. Scruby, R. J. Dewhurst, D. A. Hutchins, and S. B. Palmer, Laser Generation of Ultrasound in Metals, in *Research Techniques in Nondestructive Testing*, (1982) Vol. 5, pp. 281–327.
2. G. Birnbaum, and G. S. White, Laser Techniques in NDE, in *Research Techniques in Nondestructive Testing*, (1984) pp. 259–365.
3. D. A. Hutchins, and A. C. Tam, Pulsed Photoacoustic Materials Characterization, in *IEEE Trans. on Ultrasonics, Ferroelectrics and Frequency Control*, (1986) Vol. UFFC-33, No. 5, pp. 429–449.
4. D. A. Hutchins, Ultrasonic Generation by Pulsed Lasers, in *Physical Acoustics*, W. P. Mason and R. N. Thurston, eds., (Academic Press, NY, (1986) Vol. 18.
5. H. I. Bjelkhagen, Pulsed Fiber Holography: A New Technique for Hologram Interferometry, in *Optical Engineering*, (1985) Vol. 4, pp. 645–649.